ELSEVIER

Microelectronics Journal 30 (1999) 235–245

Microelectronics Journal

CMOS operational transresistance amplifier for analog signal processing

Khaled N. Salama[a,*], Ahmed M. Soliman[b]

[a]*Electrical Engineering Department, Stanford University, Stanford, CA, USA*
[b]*Electronics and Communications Engineering Department, Cairo University, Giza, Egypt*

Accepted 5 October 1998

Abstract

A new CMOS realization of the Operational Transresistance Amplifier (OTRA) is introduced. The properties of the OTRA are shown to be suitable for VLSI applications employing MOS transistors operating in the ohmic region. Applications of the OTRA in realizing voltage amplifiers, multipliers, integrators, continuous time filters and a quadrature oscillator are presented. Voltage mode filters that benefit from the current processing capabilities at the input terminals of the OTRA are presented. A detailed analysis taking the effect of the finite transresistance gain into consideration is provided. Both passive compensation and self-compensation of the proposed circuits are presented. The effectiveness of the proposed circuits is demonstrated through PSpice simulations based on the AMI 1.2 μm N-well level 3 parameters.

1. Introduction

Recently, current-mode analog integrated circuits in CMOS technology have received considerable interest. Current-mode techniques can achieve a considerable improvement in amplifier speed, accuracy and bandwidth, overcoming the finite gain–bandwidth product associated with operational amplifiers (op amps) [1]. Traditionally, most analog signal processing operations have been accomplished employing the voltage as the signal variable. In order to maintain compatibility with existing voltage processing circuits, it is necessary to convert the input and output signals of a current-mode signal processor to voltage using transconductors. This has the disadvantage of increasing both the chip area and power dissipation.

Current-mode circuits using the Operational Transresistance Amplifier (OTRA) as the active element suffer from using a large number of active elements [2]. This paper explores implementing voltage-mode signal processing operations using the OTRA that benefits from the current processing capabilities at the input terminals, thus reducing the number of OTRAs and keeping compatibility with existing signal processing circuits. Also, since the OTRA is not slew limited in the same fashion as op amps, it can provide amplification of high frequency signals with the ease of using standard op amps in addition to a constant bandwidth virtually independent of the gain.

The Operational Transresistance Amplifier is a three-terminal analog building block with a describing matrix in the form:

$$\begin{bmatrix} V_+ \\ V_- \\ V_o \end{bmatrix} = \begin{bmatrix} 0 & 0 & 0 \\ 0 & 0 & 0 \\ R_m & -R_m & 0 \end{bmatrix} \begin{bmatrix} I_+ \\ I_- \\ I_o \end{bmatrix} \quad (1)$$

Both the input and output terminals are characterized by low impedance, thereby eliminating response limitations incurred by capacitive time constants. The input terminals are virtually grounded leading to circuits that are insensitive to the stray capacitances [2,3]. Ideally, the transresistance gain, R_m, approaches infinity, and external negative feedback must be used which forces the input currents, I_+ and I_-, to be equal.

2. The proposed OTRA

Although the OTRA is commercially available from several manufacturers under the name current differencing or Norton amplifier, it has not gained attention until recently [4–6]. Few recent realizations have been suggested to implement the OTRA [2,7].

The proposed OTRA presented in Fig. 1 is based on the cascaded connection of the modified differential current conveyor (MDCC) [8] and a common source amplifier. The MDCC provides the current differencing operation, whereas the common source amplifier provides the high gain stage. The performance of the proposed circuit was

* Corresponding author.

0026-2692/99/$ - see front matter
PII: S0026-2692(98)00112-8

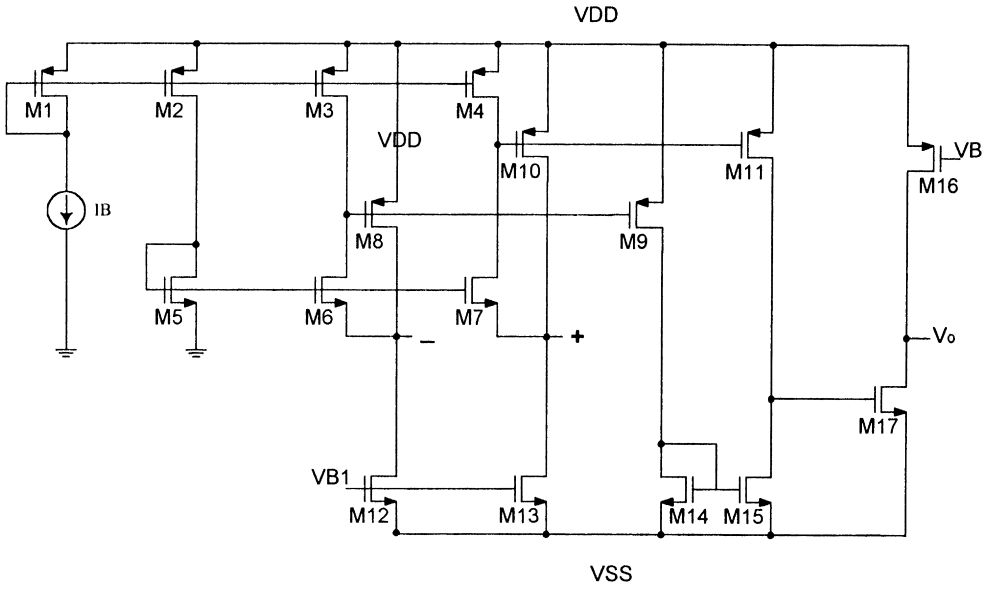

Fig. 1. Proposed CMOS realization of the OTRA.

verified by PSpice simulations, with supply voltages ±2.5 V. The output voltage of the OTRA when the non-inverting input is scanned from −200 μA to 200 μA for different values of the inverting input is shown in Fig. 2. For the proposed OTRA, the input resistance is 5 Ω, whereas the offset current is 51 nA.

For ideal operation, the transresistance gain approaches infinity and negative feedback forces the two input currents to be equal. Practically, the transresistance gain is finite and its effect should be considered. Also, the frequency limitations associated with the OTRA should be considered.

Considering a single-pole model for the transresistance gain, R_m, then:

$$R_m(s) = \frac{R_o}{1 + \frac{s}{\omega_o}} \tag{2}$$

For high frequency applications, the transresistance gain, $R_m(s)$, can be expressed as:

$$R_m(s) \approx \frac{1}{sC_p} \tag{3}$$

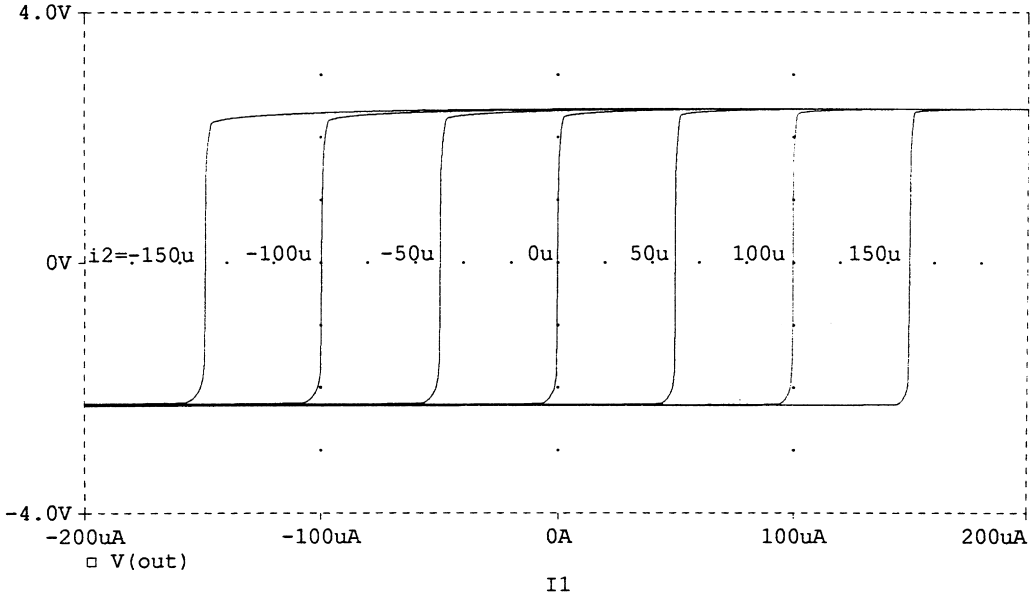

Fig. 2. Output voltage of the OTRA.

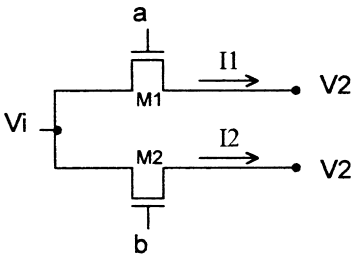

Fig. 3. Non-linearity cancellation in two matched NMOS transistor circuit.

where

$$C_p = \frac{1}{R_o \omega_o} \tag{4}$$

In the following sections, the application of the OTRA in realizing amplifiers, integrators, continuous time filters and oscillators is introduced. Methods to compensate for the finite, frequency-dependent transresistance gain, R_m, are developed. Both passive compensation and self-compensation are considered. PSpice simulation results are also included to verify analytical results.

3. Non-linearity cancellation in MOS circuits

The OTRA is suitable for non-linearity cancellation, as the two input terminals are virtually grounded. Assume that the two NMOS transistors, M1 and M2, shown in Fig. 3, are matched and operating in the ohmic region. The current in that region is given by:

$$I = K_N(V_G - V_T)(V_D - V_S) + a_1(V_D^2 - V_S^2) + a_2(V_D^3 - V_S^3) + \ldots \tag{5}$$

Since the transistors M1 and M2 have equal drain and source voltages, both the even and odd non-linearities are cancelled [9],

$$I_1 - I_2 = G(V_i - V_2) \tag{6}$$

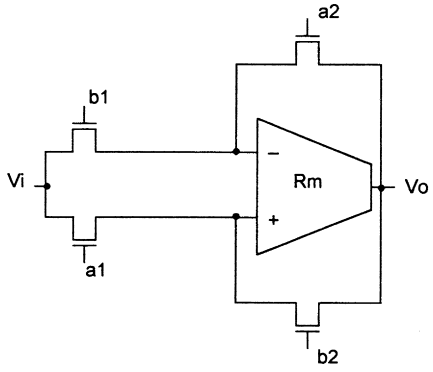

Fig. 4. OTRA-based VCVS.

where

$$G = K_N(V_a - V_b) \text{ and } K_N = \mu_N C_{ox} \frac{W}{L} \tag{7}$$

Several methods have been developed to subtract the current of MOS transistors operating in the ohmic region. In the following sections, the input terminals of the OTRA are used to achieve the subtraction operation giving rise to circuits working in the voltage mode that benefit from the current processing capabilities at the input terminals. In addition, positive and negative values of the conductance, G, can be achieved through appropriate choice of the gate control voltages V_a and V_b.

4. The OTRA-based voltage amplifier

Amplifiers find many useful applications in modern analog VLSI signal and information processing. Using linear passive resistors to achieve amplification consumes a large area. In addition, they can not be electronically programmed to compensate for the spread in their absolute values caused by random process variations. A direct application of the OTRA is to implement a Voltage Controlled Voltage Source (VCVS), as shown in Fig. 4 [10], where the output voltage is given by:

$$V_o = \frac{G_1}{G_2} V_i \tag{8}$$

where

$$G_i = K_{Ni}(V_{ai} - V_{bi}) \ (i = 1, 2) \tag{9}$$

Thus, a single OTRA is capable of providing equal gain for both the inverting and non-inverting inputs. Fig. 5 represents the frequency response for an amplifier of gain = 10. Also, it can be used as a four-quadrant multiplier/divider cell formed from a single OTRA and four MOS transistors operating in the ohmic region with no additional circuitry. Recently, analog multipliers have been used in implementing artificial neural networks [11]. A vector multiplier is shown in Fig. 6, where the output is the weighted sum of its inputs and is given by:

$$V_o = \frac{\sum_{i=1}^{n} G_i V_i}{G} \tag{10}$$

This result lends itself naturally to the VLSI implementation of Hopfield-like feedback/feedforward adaptive neural networks, where adaptive weights are realized electronically controlling the individual conductances, G_i.

Taking into consideration the finite transresistance gain, R_m, Eq. (8) of the VCVS reduces to:

$$\frac{V_o}{V_i} = \frac{G_1}{G_2} \epsilon(s) \tag{11}$$

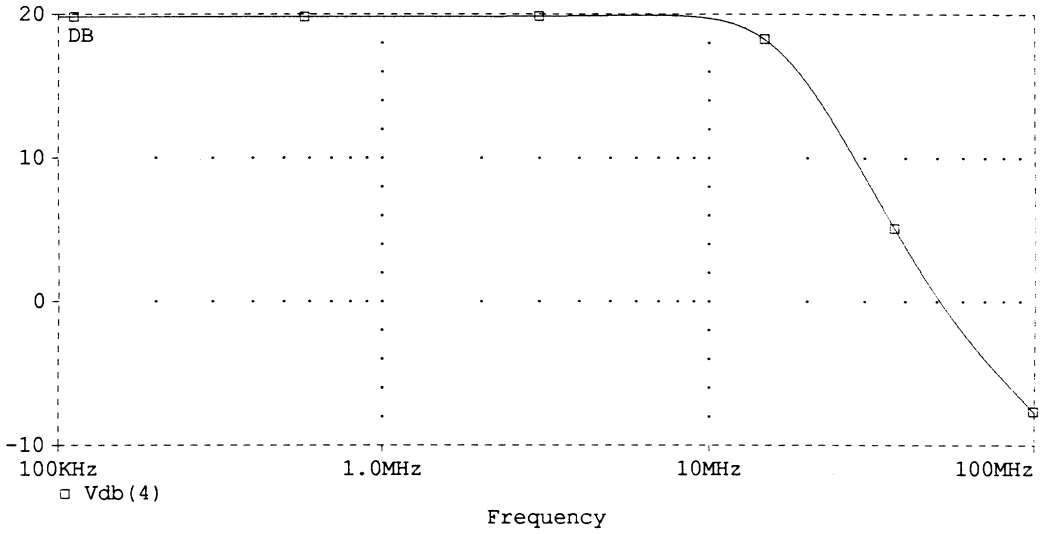

Fig. 5. Frequency spectrum of the VCVS with gain = 10.

where

$$\epsilon(s) = \frac{1}{1 + \dfrac{1}{G_2 R_m}} \tag{12}$$

For high frequency operation, the error function, $\epsilon(s)$, is given by:

$$\epsilon(s) = \frac{1}{\left(1 + \dfrac{sC_p}{G_2}\right)} \tag{13}$$

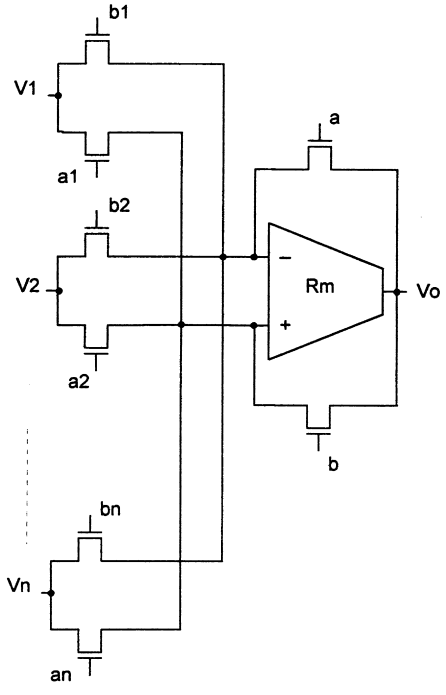

Fig. 6. Weighted summer OTRA-based circuit.

It is clear that a constant bandwidth virtually independent of the gain can be achieved by keeping the feedback conductance G_2 constant while controlling the gain through G_1. Considering the circuit shown in Fig. 7, the error function, $\epsilon(s)$, is given by:

$$\epsilon(s) = \frac{1}{\left(1 + \dfrac{sC_p - Y}{G_2}\right)} \tag{14}$$

by choosing:

$$Y = sC_p \tag{15}$$

Thus, $\epsilon(s)$ reduces to its ideal value of unity. Therefore, complete passive compensation of the VCVS can be achieved by using a single capacitor connected between the output terminal and the non-inverting terminal.

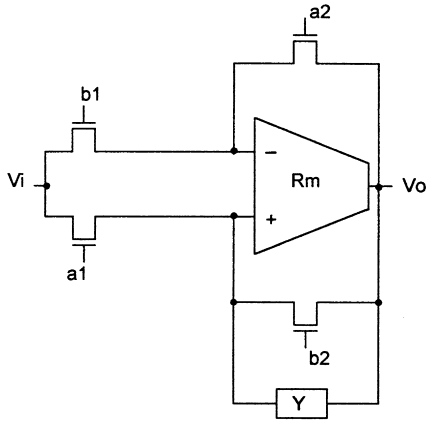

Fig. 7. Passive compensated VCVS.

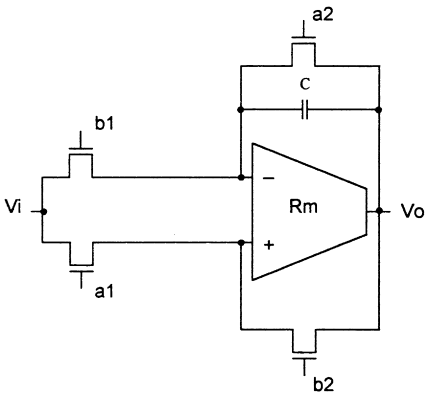

Fig. 8. Generalized voltage-mode integrator.

5. OTRA-based integrator

Current-mode and voltage-mode integrators employing a single, virtually grounded capacitor and a single OTRA are reported, respectively, in Refs [2,10,12]. A new generalized voltage-mode integrator is shown in Fig. 8. The proposed integrator can be tuned to achieve both ideal and lossy integration. The transfer function is given by:

$$\frac{V_o}{V_i} = \frac{G_1}{G_2}\frac{1}{\left(\frac{s}{\omega_o} + 1\right)} \tag{16}$$

where

$$\omega_o = \frac{G_2}{C} \tag{17}$$

Thus, ideal integration can be achieved by setting, $G_2 = 0$, and by equating the gate control voltages, V_{a2} and V_{b2}. Practically, this is equivalent to removing the two NMOS transistors in the feedback paths. Taking into consideration the effect of the transresistance gain, R_m, for the integrator circuit shown in Fig. 8, Eq. (17) reduces to:

$$\omega_o = \frac{G_2}{(C_p + C)} \tag{18}$$

Thus, the integrating capacitor, C, is chosen to be much larger than C_p in order to eliminate its effect. It is also possible to compensate the effect of C_p, by taking the design value of C equal to its theoretical value minus C_p. Self-compensation can be achieved by using a capacitor, C', where

$$C' = C - C_p \tag{19}$$

Thus, the effect of C_p is absorbed in the integrating capacitance C' and no additional elements for compensation are needed.

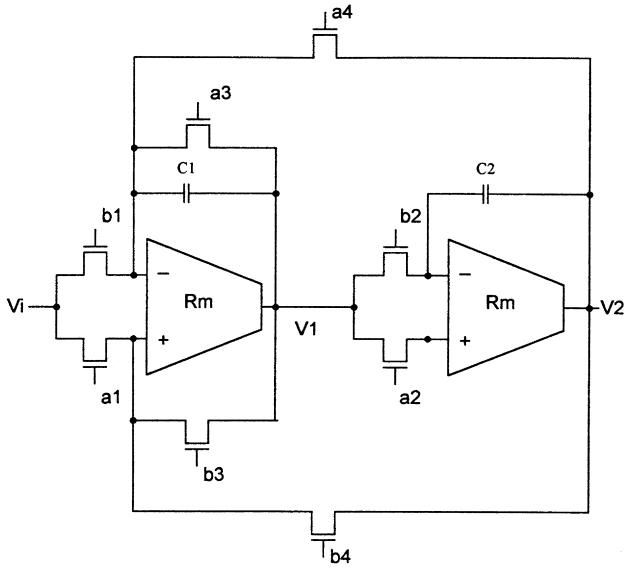

Fig. 9. The TT biquad circuit.

6. Continuous time active filters

Continuous time filters using op amps, transconductors and switched capacitors are now widely accepted in industry where they are used in applications involving direct signal processing, especially for medium dynamic range applications [1,13]. Recently, filters with low power dissipation and high frequency operation using current mirrors [14], voltage followers [15], Current Feedback Operational Amplifiers [16] or Operational Transresistance Amplifiers [2] have been developed to overcome the finite gain–bandwidth product associated with traditional operational amplifiers.

Usually, two inverting integrators are cascaded and a third inverter allows the closing of the overall loop with the proper phase. This idea is behind many of the biquad filter structures available. The active element count in these structures can be reduced, if a true non-inverting integrator could be built with a single active element [5]. Unfortunately, this cannot be done with single input op amps, but easily done using the OTRA. In addition, the availability of two virtual ground terminals at the input of the OTRA allows for summing currents leading to circuits with a lower number of active elements.

The realization of the Tow Thomas (TT) biquad, the Kerwin–Huelsman–Newcomb Biquad (KHN) biquad and a universal filter are introduced in the following subsections.

6.1. The Tow Thomas biquad

Since the TT biquad depends on current summing by introducing a virtual ground at the input terminal of the conventional op amp and the availability of performing only inverting integration, three op amps are needed. On the other hand, since the OTRA does not suffer from these problems, the TT biquad can be implemented, as shown in Fig. 9, using only two OTRAs [10]. All possible polarities of the bandpass and lowpass outputs are summarized in Table 1. The transfer function of the bandpass and the lowpass

Table 1
The four alternative response polarities of the TT biquad

G_i polarity				Filter response polarity	
G_1	G_2	G_3	G_4	BP	LP
+	+	+	+	+	+
+	−	+	−	+	−
−	−	+	−	−	+
−	+	+	+	−	−

outputs are given by:

$$\frac{V_1}{V_i} = \frac{\frac{G_1 s}{C_1}}{D(s)} \text{ and } \frac{V_2}{V_i} = \frac{\frac{G_1 G_2}{C_1 C_2}}{D(s)} \tag{20}$$

where $D(s)$ is given by:

$$D(s) = s^2 + \frac{G_3}{C_1}s + \frac{G_2 G_4}{C_1 C_2} \tag{21}$$

Thus, ω_o and Q are given by:

$$\omega_o = \sqrt{\frac{G_2 G_4}{C_1 C_2}} \text{ and } Q = \frac{1}{G_3}\sqrt{\frac{C_1 G_2 G_4}{C_2}} \tag{22}$$

For a lowpass response with a specified DC gain, $|T(0)|$;

$$G_1 = |T(0)|G_4 \tag{23}$$

For a bandpass response with a specified center frequency gain, $|T(j\omega_o)|$,

$$G_1 = |T(j\omega_o)|G_3 \tag{24}$$

High-Q integrated circuit bandpass filters remain an interesting general design objective [3]. It is clear from Eq. (22) that the quality factor Q can be independently controlled without affecting ω_o by varying G_3. Also, the conductance G_1 controls the filter gain without affecting either ω_o or Q. The TT biquad filter is self-compensated by absorbing the effect of the stray capacitance C_p presented in both C_1 and C_2, and no additional elements for compensation are needed.

Table 2
The eight alternative response polarities of the KHN biquad

G_i polarity						Filter response polarity		
G_1	G_2	G_3	G_4	G_5	G_6	HP	BP	LP
+	+	+	+	+	+	+	+	+
+	+	−	+	+	−	+	+	−
+	−	−	+	−	+	+	−	+
+	−	+	+	−	−	+	−	−
−	−	+	+	−	−	−	+	+
−	−	−	+	−	+	−	+	−
−	+	−	+	+	−	−	−	+
−	+	+	+	+	+	−	−	−

Fig. 10 represents the ideal and simulated lowpass response of the TT biquad designed to give a Butterworth response, where:$C_1 = C_2 = 20$ pF, $G_1 = G_2 = G_4 = 142.2$ μA/V and $G_3 = 201.924$ μA/V.

6.2. The Kerwin–Huelsman–Newcomb biquad

Unlike the classical KHN biquad [17], all possible combinations of polarities of the highpass, bandpass and lowpass responses can be obtained as indicated in Table 2 for the circuit shown in Fig. 11. The transfer functions of the highpass, bandpass and lowpass outputs are given by:

$$\frac{V_1}{V_i} = \frac{\frac{G_1 s^2}{G_4}}{D(s)}, \frac{V_2}{V_i} = \frac{\frac{G_1 G_2 s}{G_4 C_1}}{D(s)} \text{ and } \frac{V_3}{V_i} = \frac{\frac{G_1 G_2 G_3}{G_4 C_1 C_2}}{D(s)} \tag{25}$$

where $D(s)$ is given by:

$$D(s) = s^2 + \frac{G_2 G_5}{G_4 C_1}s + \frac{G_2 G_3 G_6}{G_4 C_1 C_2} \tag{26}$$

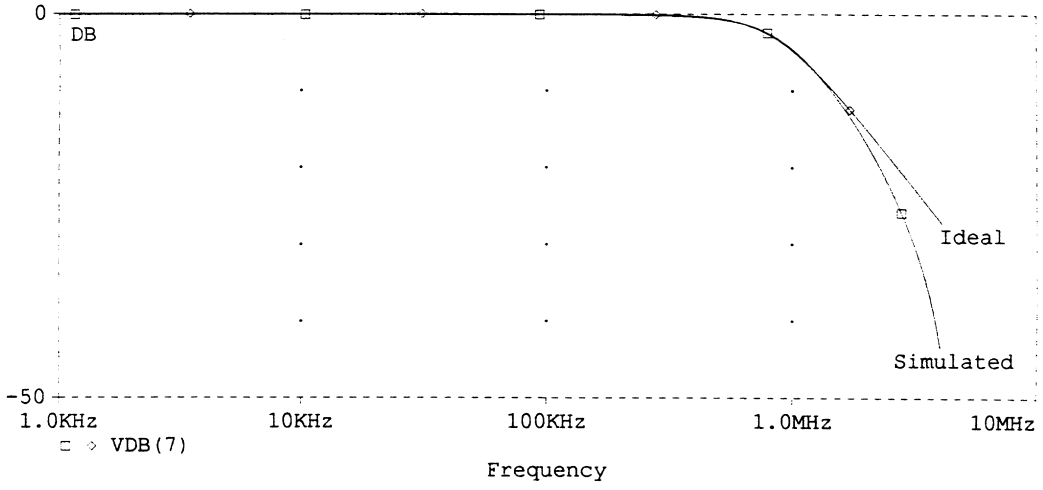

Fig. 10. Ideal and simulated responses for a Butterworth lowpass filter.

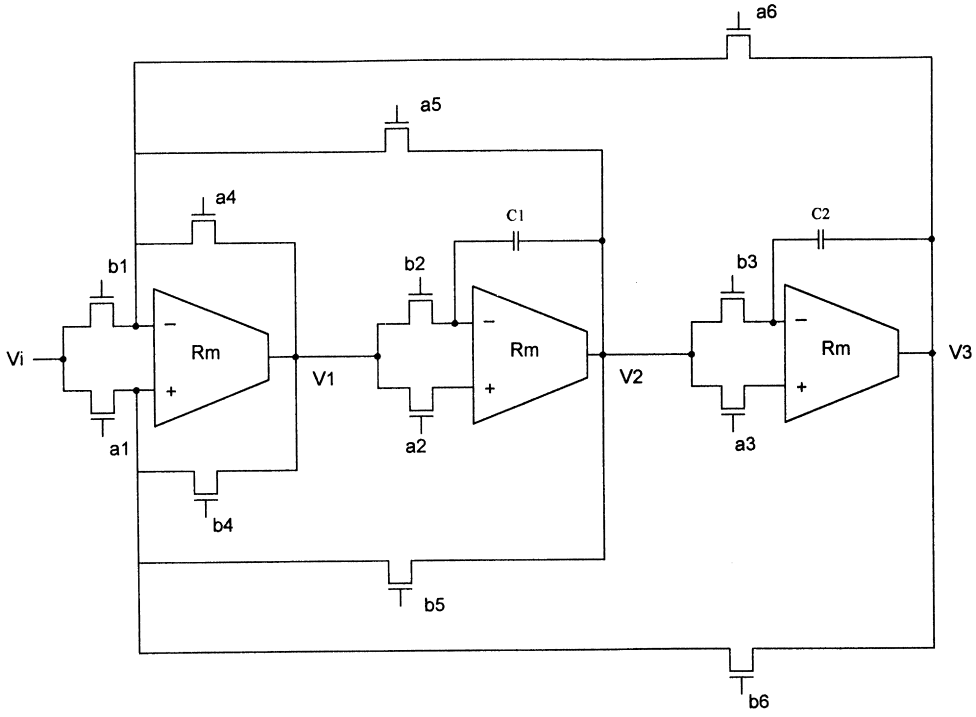

Fig. 11. The KHN biquad circuit.

Thus, ω_o and Q are given by:

$$\omega_o = \sqrt{\frac{G_2 G_3 G_6}{G_4 C_1 C_2}} \text{ and } Q = \frac{1}{G_5}\sqrt{\frac{C_1 G_3 G_4 G_6}{C_2 G_2}} \tag{27}$$

For a lowpass response with a specified DC gain, $|T(0)|$;

$$G_1 = |T(0)|G_6 \tag{28}$$

For a bandpass response with a specified center frequency gain, $|T(j\omega_o)|$;

$$G_1 = |T(j\omega_o)|G_5 \tag{29}$$

For a highpass response with a specified gain, $|T(\infty)|$;

$$G_1 = |T(\infty)|G_4 \tag{30}$$

It is clear that the quality factor Q can be independently controlled by varying G_5 without affecting ω_o. It is also seen that the conductance G_1 controls the filter gain without

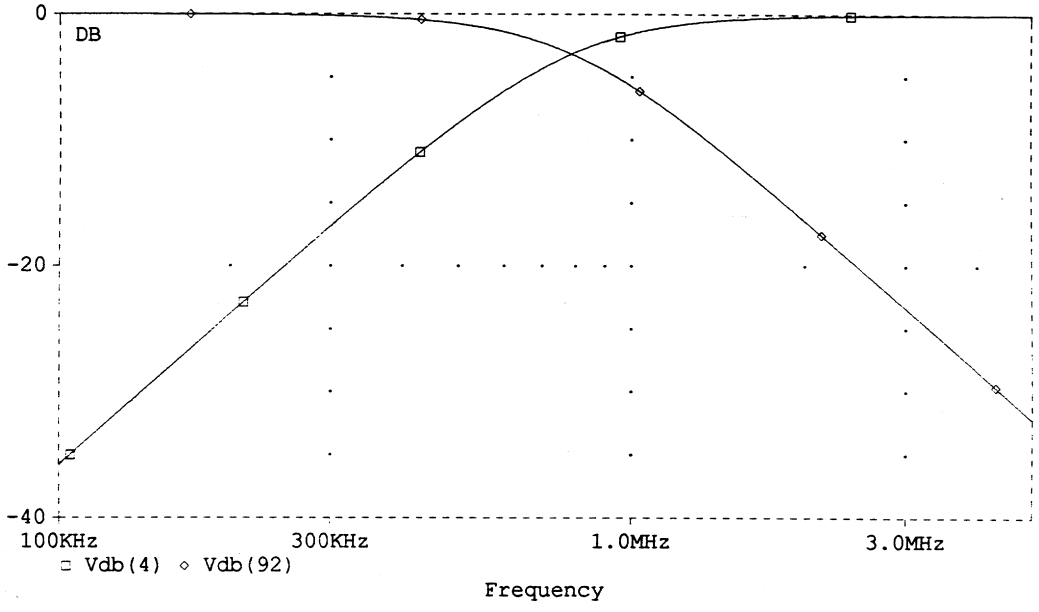

Fig. 12. Highpass and lowpass responses of the KHN biquad.

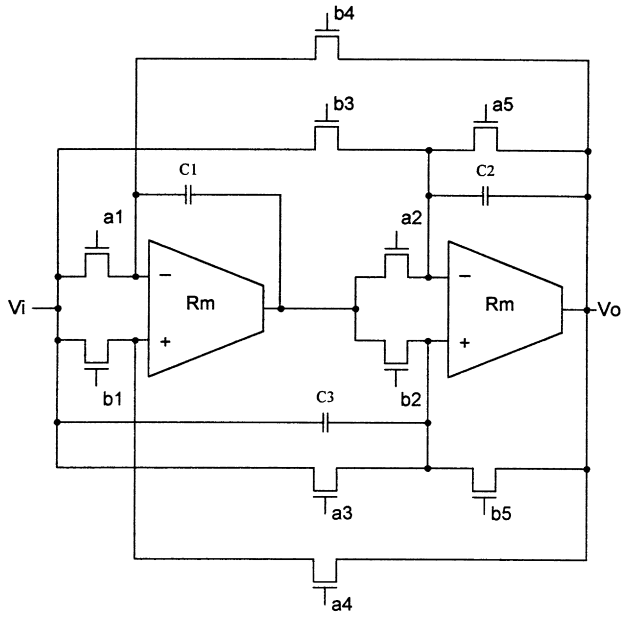

Fig. 13. Second order universal filter.

Table 3
The realizability conditions for the universal filter of Fig. 13

Filter response	Realizability condition
Highpass	$G_3 = G_1 = 0$
Bandpass	$C_3 = 0$, $G_1 = 0$
Lowpass	$C_3 = 0$, $G_3 = 0$
All pass	$G_3 = -G_5$, $C_3 = C_2$, $G_1 = G_4$
Notch	$G_3 = 0$, $C_3 = C_2$, $G_1 = G_4$

affecting ω_o or Q, an advantage which does not exist in the classical KHN circuit using op amps [17]. Compensation can be achieved by using a single capacitor, C_p, connected between the output terminal and the non-inverting terminal of the first OTRA employed as a weighted summer; whereas the effect of the stray capacitance, C_p, in the other two OTRAs used as ideal integrators can be absorbed in the integrating capacitors C_1 and C_2.

Fig. 12 represents the lowpass and highpass responses designed to give a Butterworth response, where: $C_1 = C_2 = 10$ pF, $G_1 = G_2 = G_3 = G_4 = G_6 = 63.06$ μA/V and $G_5 = 89.54$ μA/V.

6.3. Universal filter

Second order universal filters are designed to provide lowpass, bandpass, highpass, all pass and notch responses. Two current mode universal filters, each employing three OTRAs, are presented in Ref. [2]. A novel voltage-mode universal filter that uses a minimum number of active elements is presented in Fig. 13. The transfer function is given by:

$$\frac{V_o}{V_i} = \frac{\frac{C_3}{C_2}s^2 + \frac{G_3}{C_2}s + \frac{G_1G_2}{C_1C_2}}{D(s)} \tag{31}$$

where $D(s)$ is given by:

$$D(s) = s^2 + \frac{G_5}{C_2}s + \frac{G_2G_4}{C_1C_2} \tag{32}$$

Thus ω_o and Q are given by:

$$\omega_o = \sqrt{\frac{G_2G_4}{C_1C_2}} \text{ and } Q = \frac{1}{G_5}\sqrt{\frac{C_2G_2G_4}{C_1}} \tag{33}$$

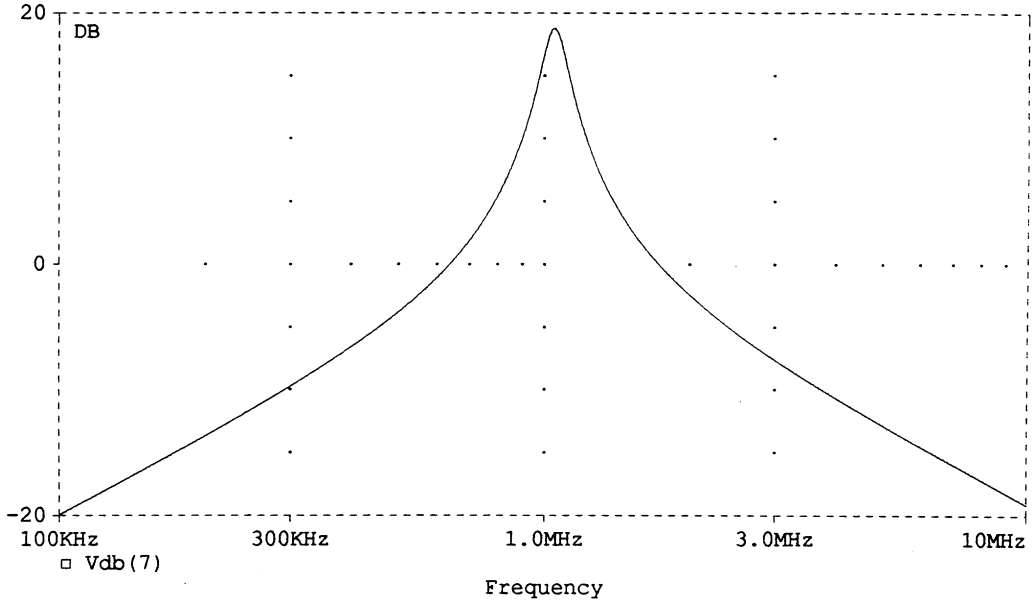

Fig. 14. Bandpass response with $Q = 10$.

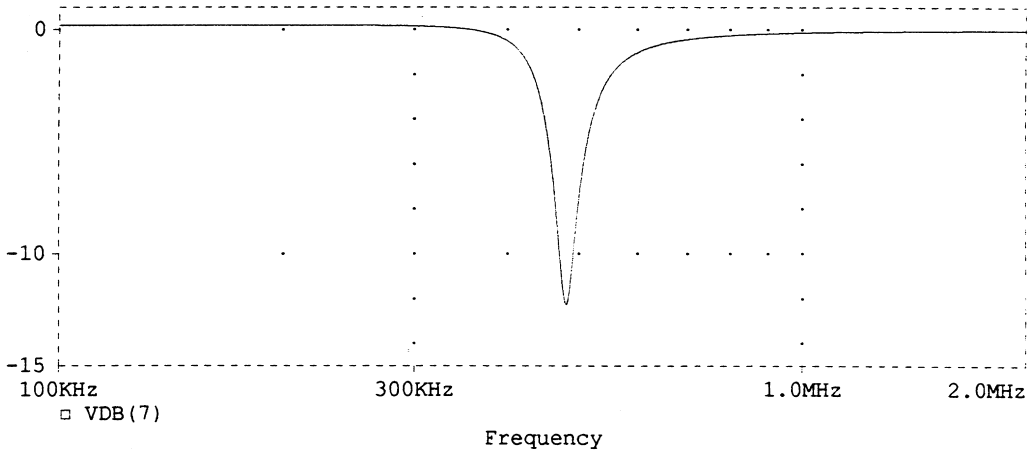

Fig. 15. Band stop response of the universal filter.

It is clear that the quality factor Q can be independently controlled by varying G_5 without affecting ω_o. All possible outputs are summarized in Table 3. The proposed configuration is attractive in realizing higher order transfer functions. An n-order filter based on this configuration requires only n OTRAs.

Again, the proposed universal filter is self-compensated since the effect of the stray capacitance C_p can be absorbed in both C_1 and C_2.

Fig. 14 represents the positive bandpass response of the filter designed to give $Q = 10$, where: $C_1 = C_2 = 10$ pF, $G_2 = G_3 = G_4 = 79$ μA/V and $G_5 = 7.9$ μA/V.

Fig. 15 represents the magnitude of a notch filter having: $C_1 = C_2 = C_3 = 10$ pF, $G_1 = G_2 = G_4 = 41.47$ μA/V and $G_5 = 4.14$ μA/V.

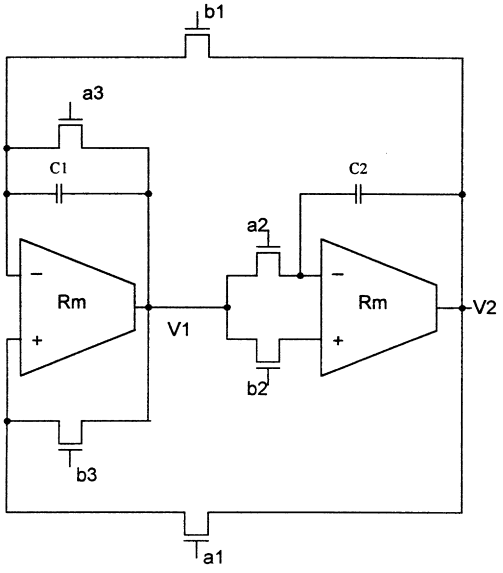

Fig. 16. Quadrature oscillator circuit.

7. Quadrature oscillator

A novel quadrature oscillator is presented in Fig. 16. To the best of the authors' knowledge, this is the first oscillator using the OTRA. The characteristic equation is given by:

$$s^2 + \frac{G_3}{C_1}s + \frac{G_1G_2}{C_1C_2} = 0 \tag{34}$$

Thus, the circuit represents a minimal component virtually grounded capacitor oscillator with independent control on the condition of oscillation as described by:

$$G_3 = 0 \tag{35}$$

It is seen that the conductance, G_3, controls the condition of oscillation without affecting the radian frequency of oscillation, which is given by:

$$\omega_o = \sqrt{\frac{G_1G_2}{C_1C_2}} \tag{36}$$

Thus, the radian frequency can be controlled through adjusting G_1 or G_2 through appropriate choice of any of the gate control voltages, V_{a1}, V_{a2}, V_{b1} and V_{b2}, without affecting the oscillation condition which is controlled by either V_{a3} or V_{b3}.

The passive sensitivities of this oscillator are all low and are given by:

$$S_{G_1}^{\omega_o} = S_{G_2}^{\omega_o} = -S_{C_1}^{\omega_o} = -S_{C_2}^{\omega_o} = \frac{1}{2} \tag{37}$$

If the effect of the finite transresistance gain, R_m, was considered, then Eq. (34) reduces to:

$$s^2 + \frac{G_3}{(C_1 + C_p)}s + \frac{G_1G_2}{(C_1 + C_p)(C_2 + C_p)} = 0 \tag{38}$$

Thus, the effect of C_p can be absorbed in C_1 and C_2 without increasing the order of the circuit.

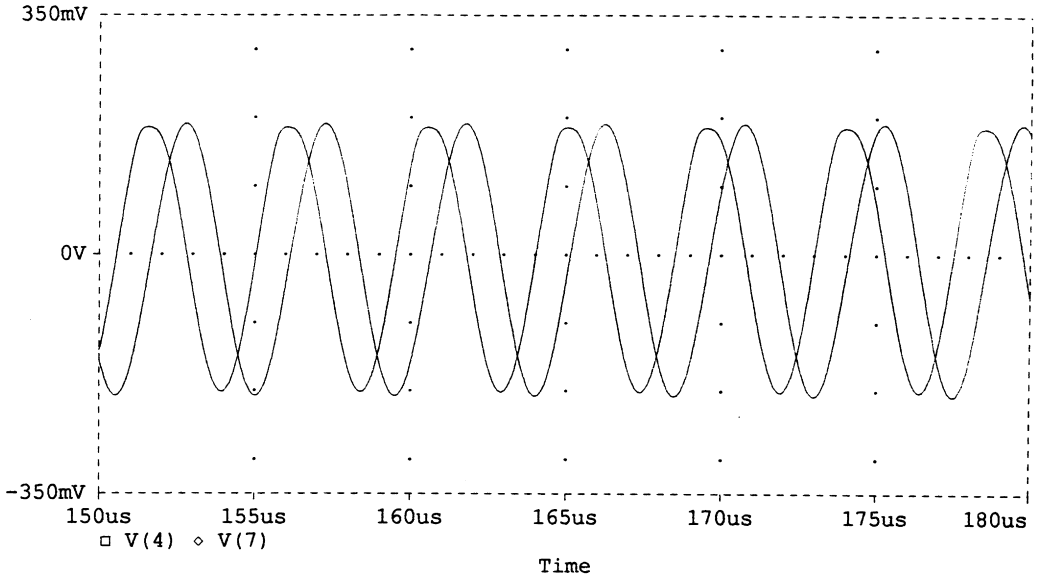

Fig. 17. Oscillator output waveform.

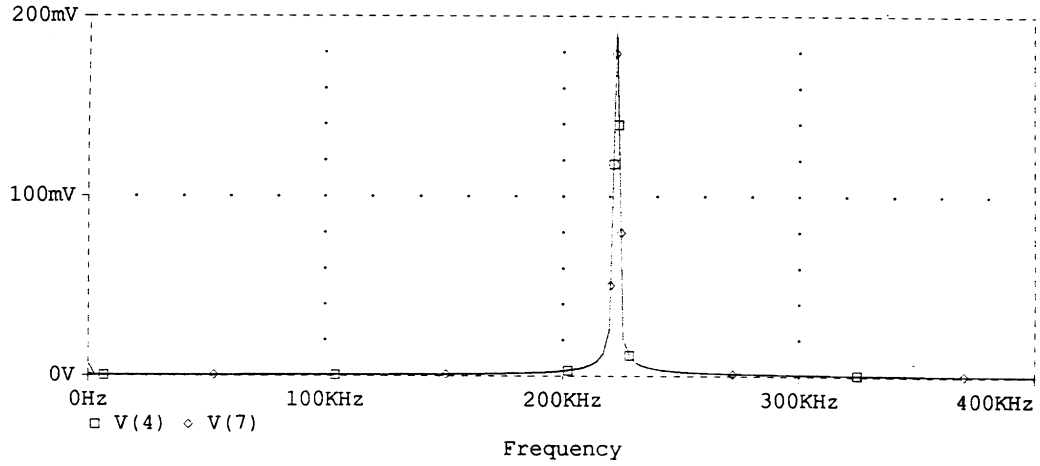

Fig. 18. Oscillator frequency spectrum.

Figs. 17 and 18 represent the output waveform and frequency spectrum of the oscillator two outputs with $G_1 = G_2 = 142.2$ μA/V and $C_1 = C_2 = 100$ pF. To start oscillations, the control voltages V_{a3} and V_{b3} were adjusted such that $V_{a3} - V_{b3} = 0.1$ V and thus $G_3 = 14.2$ μA/V. From simulations, $f_0 = 222.875$ kHz: thus $\Delta f_0/f_0 = -1.52\%$ and the THD = 2.6%.

8. Conclusions

A new realization of the Operational Transresistance Amplifier is presented. The OTRA provides a constant bandwidth virtually independent of the gain. The main advantage of the OTRA is the ability to implement different analog circuits without the need of resistors, as it can be used to cancel both the even and odd non-linear terms associated with MOS transistors operating in the ohmic region. The proposed applications, which employ this concept, are MOS-C amplifiers, integrators, continuous time filters and oscillators. The effect of the finite transresistance gain is considered and methods for compensation have been proposed. PSpice simulations that confirm the theoretical analysis are included.

References

[1] C. Toumazou, F. Lidgey, D. Haigh, Analogue IC Design: the Current-Mode Approach, Peter Peregrinus, 1990.
[2] J. Chen, H. Tsao, S. Liu, W. Chui, Parasitic-capacitance-insensitive current-mode filters using operational transresistance amplifiers, IEE Proc. Circuits Devices and Systems 142 (3) (1995) 186–192.
[3] J. Choma, Communication circuits: societal philosophies and evolving roles. IEEE Circuits and Systems Society Newsletter 9(2) (1998).

[4] J. Brodie, A notch filter employing current differencing operational amplifier, International Journal of Electronics 41 (5) (1976) 501–508.
[5] National Semiconductor Corp., Designing with a New Super Fast Dual Norton Amplifier, Linear Applications Data Book, 1981.
[6] National Semiconductor Corp., The LM3900: A New Current Differencing ± Quad of the Input Amplifiers, Linear Applications Data Book, 1986.
[7] J. Chen, H. Tsao, C. Chen, Operational transresistance amplifier using CMOS technology, Electron. Lett. 28 (22) (1992) 2087–2088.
[8] H.O. Elwan, A.M. Soliman, CMOS differential current conveyors and applications for analog VLSI, Analog Integrated Circuits and Signal Processing 11 (5) (1996) 35–45.
[9] M. Ismail, T. Fiez, Analog VLSI Signal and Information Processing, McGraw-Hill, New York, 1994.
[10] H.O. Elwan, CMOS current mode circuits and applications for analog VLSI. M.Sc. thesis, Cairo University, 1996.
[11] C. Mead, M. Ismail, Analog VLSI Implementation of Neural Systems, Kluwer Academic, Boston, 1989.
[12] W. Chui, J. Tsay, S. Liu, H. Tsao, J. Chen, Single-capacitor MOSFET-C integrator using OTRA, Electron. Lett. 31 (21) (1995) 1796–1797.
[13] S. Lee, R. Zele, D. Allstot, G. Liang, CMOS continuous-time current-mode filters for high frequency applications, IEEE J. Solid State Circuits 28 (1993) 323–329.
[14] R. Zele, D. Allstot, T. Fiez, Fully balanced CMOS current-mode circuits, IEEE J. Solid State Circuits 28 (5) (1993) 569–575.
[15] Y. Tsividis, Y. Papananos, Continuous-time filters using buffers with gain lower than unity, Electron. Lett. 30 (8) (1994) 629–630.
[16] A.M. Soliman, Applications of the current feedback operational amplifiers, Analog Integrated Circuits and Signal Processing 11 (1996) 265–301.
[17] W. Kerwin, L. Huelsman, R. Newcomb, State variable synthesis for insensitive integrated circuit transfer functions, IEEE J. Solid State Circuits 2 (1967) 87–92.